Inorganic Chemistry

Article

pubs.acs.org/IC

Multinuclear Solid-State NMR and DFT Studies on Phosphanido-Bridged Diplatinum Complexes

Piero Mastrorilli,*[,†,‡] Stefano Todisco,[†] Alessandro Bagno,[§,¶] Vito Gallo,[†] Mario Latronico,[†,‡] Consuelo Fortuño,[∥] and Dietrich Gudat[⊥]

[†]Dipartimento di Ingegneria Civile, Ambientale, del Territorio, Edile e di Chimica (DICATECh), Politecnico di Bari, Via Orabona 4, I-70125 Bari, Italy

[‡]Consiglio Nazionale delle Ricerche, Istituto di Chimica dei Composti Organometallici (ICCOM-CNR), Via Orabona 4, 70125 Bari, Italy

[§]Dipartimento di Scienze Chimiche, Università di Padova, Via Marzolo 1, 35131 Padova, Italy

[∥]Departamento de Química Inorgánica, Instituto de Síntesis Química y Catálisis Homogénea, Universidad de Zaragoza-C.S.I.C., E-50009 Zaragoza, Spain

[⊥]Institut für Anorganische Chemie, Universität Stuttgart, Pfaffenwaldring 55, 70569 Stuttgart, Germany

Supporting Information

ABSTRACT: Multinuclear (^{31}P, ^{195}Pt, ^{19}F) solid-state NMR experiments on $(n\mathrm{Bu_4N})_2[(C_6F_5)_2Pt(\mu\text{-}PPh_2)_2Pt(C_6F_5)_2]$ (**1**), $[(C_6F_5)_2Pt(\mu\text{-}PPh_2)_2Pt(C_6F_5)_2]$ (*Pt−Pt*) (**2**), and *cis*-$Pt(C_6F_5)_2(PHPh_2)_2$ (**3**) were carried out under cross-polarization/magic-angle-spinning conditions or with the cross-polarization/Carr−Purcell Meiboom−Gill pulse sequence. Analysis of the principal components of the ^{31}P and ^{195}Pt chemical shift (CS) tensors of **1** and **2** reveals that the variations observed comparing the isotropic chemical shifts of **1** and **2**, commonly referred to as "ring effect", are mainly due to changes in the principal components oriented along the direction perpendicular to the Pt_2P_2 plane. DFT calculations of ^{31}P and ^{195}Pt CS tensors confirmed the tensor orientation proposed from experimental data and symmetry arguments and revealed that the different values of the isotropic shieldings stem from differences in the paramagnetic and spin−orbit contributions.

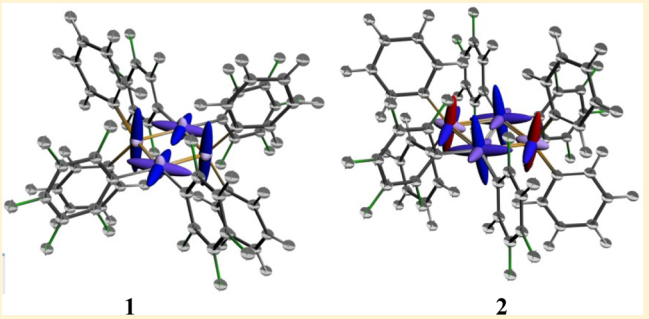

INTRODUCTION

Platinum diorganophosphanido complexes have been the object of intense study in the last years due to the rich chemistry they exhibit.[1−19] NMR spectroscopy is a powerful technique for investigating the structure and dynamics in solution of such complexes, owing to the presence of several different spin 1/2 nuclei in these molecules (^{1}H, ^{31}P, ^{195}Pt, ^{13}C, and in several cases ^{19}F). Although NMR studies on this kind of complexes have been performed for several decades, some issues about ^{195}Pt NMR and ^{31}P NMR remain unclear.

It has been long known that the ^{31}P chemical shift of bridging diorganophosphanides is particularly sensitive to its electronic environment as modified by the nature of the Pt−Pt bond (this effect occurs for other dimetal diorganophosphanido complexes).[20−22] In particular, when the R_2P group bridges two nonbonded Pt atoms forming a four-membered Pt−P−Pt−X ring (X = P, N, O, Cl, Br, I), the ^{31}P chemical shift ranges from +5 to −260 ppm (Chart 1, structures G and H); the open bridge R_2P group and the R_2P group bridging two nonbonded Pt atoms forming a five-membered Pt−P−Pt−P−X ring (X = N, O) are characterized by ^{31}P chemical shift values ranging from −20 to 50 ppm (Chart 1, E and F); when the R_2P group subtends a Pt−Pt bond (Chart 1, A, B, C, D), the ^{31}P chemical shifts of the diorganophosphanide involved in the three-membered Pt_2P ring range from 90 to 400 ppm.

As for the ^{195}Pt NMR, the simplest distinction that one can make is among the different oxidation states exhibited by these complexes, ^{195}Pt nuclei in Pt(II) complexes being generally much more shielded than in Pt(IV) ones.[23−26] However, this simplification does not hold for platinum diorganophosphanido complexes. In fact, as shown in Chart 2, such compounds exist with Pt atoms exhibiting formal oxidation states of +1, +2, +3, and +4, and, even though only a few examples are reported for μ-PR_2 Pt complexes in the oxidation states +3 and +4, no regular trend correlating the chemical shift with the Pt oxidation state can be observed.

Diorganophosphanido-bridged species bearing Pt(IV) are rare, the only examples available in the literature being constituted by mixed-valence Pt(II)/Pt(IV) complexes (Chart

Received: March 19, 2015
Published: May 22, 2015

DOI: 10.1021/acs.inorgchem.5b00627
Inorg. Chem. 2015, 54, 5855−5863

Chart 1. Ranges of ^{31}P Chemical Shifts for Diorganophosphanido Platinum Complexes

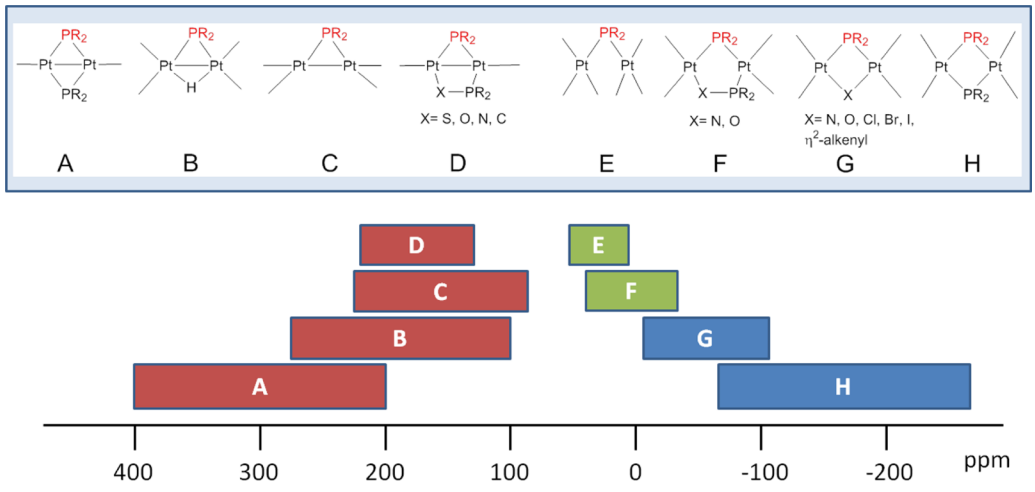

Chart 2. Ranges of ^{195}Pt Chemical Shifts for Diorganophosphanido Platinum Complexes

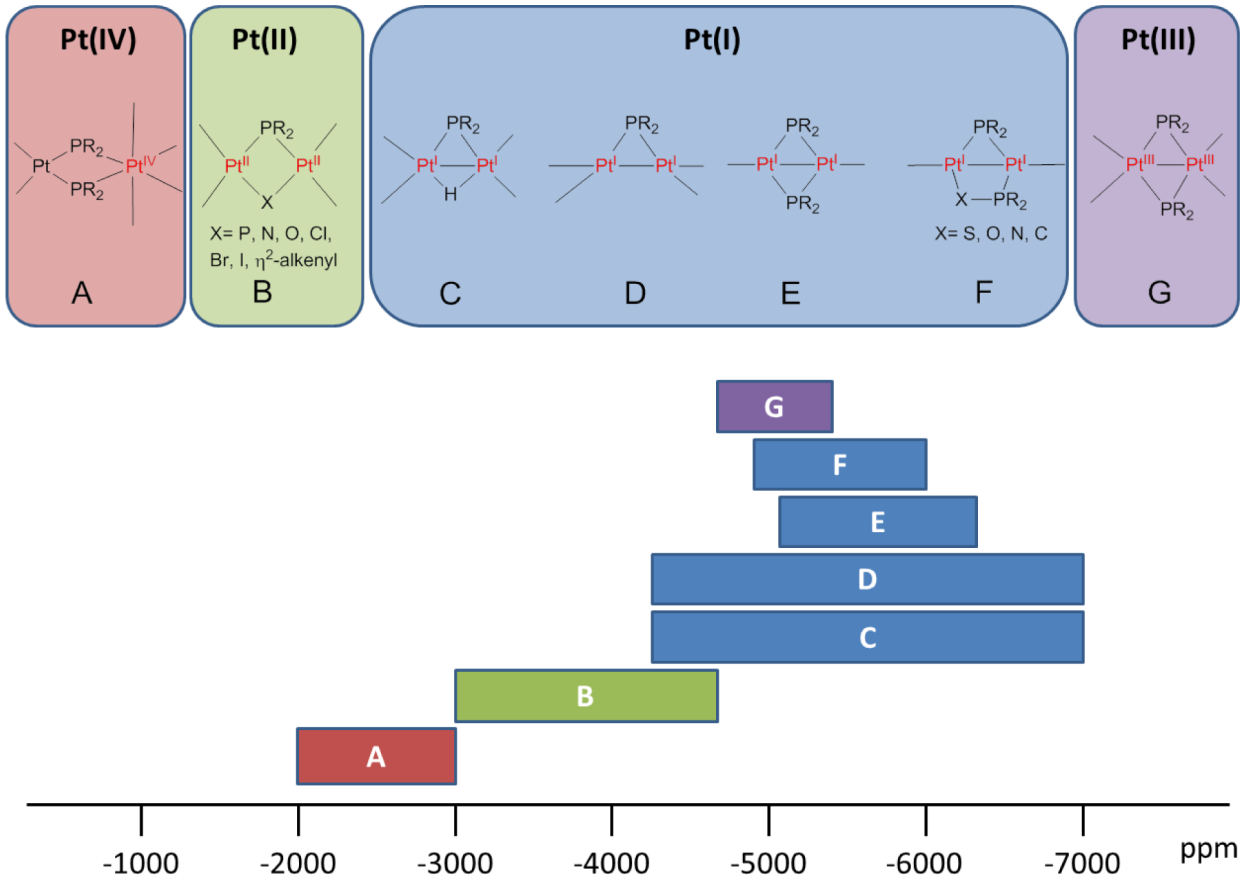

2, A) where the Pt(IV) exhibits ^{195}Pt chemical shifts ranging from −2000 to −3000 ppm. Diorganophosphanido complexes of Pt(III) are also quite rare and show $\delta_{Pt(III)}$ ranging from −4700 to −5300 ppm (Chart 2, G). A large number of phosphanido-bridged species bearing Pt(II) have been described (Chart 2, B), and their ^{195}Pt chemical shifts range from −3000 to −4700 ppm. If the change in shielding observed comparing Pt(IV) with Pt(III) looks reasonable on the basis of a higher electron density around the Pt nucleus expected upon decreasing the Pt oxidation state, the values observed for Pt(II) are not immediately rationalized. The known Pt(I) dimers described in the literature[27] exhibit ^{195}Pt chemical shifts ranging from −4200 to −6900 ppm (Chart 2, C−F), in the region where diorganophosphanido Pt(III) complexes are observed. It should also be remarked that correlations between atomic charges and chemical shifts are of limited scope and may exhibit counterintuitive trends.[28]

It is known that the total shielding of a heavy nucleus can be partitioned into the sum of diamagnetic (σ_d), paramagnetic (σ_p), and spin−orbit contributions (σ_{SO}) (eq 1).[29] In the case of ^{31}P, the paramagnetic contribution (σ_p) is thought to be predominant in the total shielding,[30] while, in the case of ^{195}Pt,

DOI: 10.1021/acs.inorgchem.5b00627
Inorg. Chem. 2015, 54, 5855−5863

both the paramagnetic and the relativistic spin−orbit terms were demonstrated to contribute substantially.[31]

$$\sigma = \sigma_d + \sigma_p + \sigma_{SO} \quad (1)$$

Given that σ_p (which exerts the dominant influence on ^{31}P shielding) depends on the energy difference between excited and ground states,[29] the strong deshielding observed for the ^{31}P resonance upon going from structures having μ-PR_2 involved in three-membered rings (A−D in Chart 1) to structures having μ-PR_2 involved in four-membered rings (G and H in Chart 1) has been interpreted in terms of a smaller gap between the highest occupied molecular orbital (HOMO) and the lowest unoccupied molecular orbital (LUMO).[32]

The trends reported in Charts 1 and 2 show that, on passing from Pt−Pt bonded species to Pt···Pt "nonbonded" ones, the ^{31}P nuclei are strongly shielded, while the ^{195}Pt nuclei become more deshielded. This calls the simple correlation of the paramagnetic shielding with a HOMO−LUMO gap into question,[33] because such an influence would result in parallel trends for ^{31}P and ^{195}Pt nuclei. Therefore, in order to gain insights into the different contributions to the total ^{31}P and ^{195}Pt shielding and the three-dimensional nature of the shielding for a diorganophosphanido-bridged Pt complex either with or without a Pt−Pt bond, we decided to carry out an experimental and theoretical solid-state multinuclear NMR study on complex $(n\mathrm{Bu_4N})_2[(C_6F_5)_2Pt(\mu\text{-}PPh_2)_2Pt(C_6F_5)_2]$ (**1**) and its two-electron oxidation product $[(C_6F_5)_2Pt(\mu\text{-}PPh_2)_2Pt(C_6F_5)_2]$(*Pt−Pt*) (**2**). These two complexes, whose XRD structures are known, possess pairs of ^{31}P and ^{195}Pt nuclei that are chemically equivalent in solution, differ in the formal Pt oxidation states (as a consequence of the different total number of electrons), and have very similar structures, the main difference being the shape of the Pt_2P_2 ring, which is elongated in the Pt−Pt direction in the case of **1** (Chart 3). The study has been complemented with the mononuclear complex *cis*-$Pt(C_6F_5)_2(PHPh_2)_2$ (**3**), which can be considered a "building block" of **1** and **2** and in which the coordination around the Pt atom is essentially the same as in **1** but with two terminally bonded diphenylphosphanes in place of the bridging diphenylphosphanides.

Chart 3

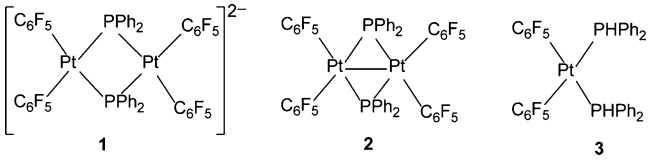

EXPERIMENTAL SECTION

Complexes **1**,[34] **2**,[35] and **3**[34] were prepared by literature methods.

Solid-State NMR. Solid-state NMR experiments were performed on a Bruker Avance I 400 spectrometer using a 4.0 mm HX MAS probe at 298 K. For MAS and static (nonspinning) experiments, samples were packed in zirconia rotors. Chemical shifts are referenced to H_2PtCl_6 (^{195}Pt, 86.0 MHz), H_3PO_4 (^{31}P, 161.9 MHz), and $CFCl_3$ (^{19}F, 376.5 MHz). For ^{31}P and ^{195}Pt NMR spectra, a two-pulse phase-modulation decoupling scheme was used for the ^{1}H decoupling.

^{1}H−^{31}P CP/MAS NMR experiments were performed using a 3.25 μs proton $\pi/2$ pulse length, a ν_{CP} of 55.0 kHz, a contact time of 5.0 ms, a ν_{dec} of 76.9 kHz, and a recycle delay of 6 s. ^{1}H−^{31}P CP/MAS NMR spectra of complexes **1** and **2** were acquired collecting two subspectra using a spectral width of 75.2 kHz for **1** and 64.9 kHz for **2**. The transmitter offsets were set at 0 and −75 188 Hz for **1** and 89 087 and 26 726 Hz for **2**. The line width at half-height of the peaks was ca. 475 Hz for **1** and 220 Hz for **2**. For the static experiments, ^{195}Pt powder patterns were acquired by collecting subspectra with a spectral width of 75 kHz[36,37] and 60 Meiboom−Gill (MG) loops. For complex **1**, 16 subspectra were acquired using transmitter offsets spaced by 24.9 kHz (the first transmitter offset was set at −498 887 Hz), for complex **2** four subspectra spaced by 25.8 kHz (the first transmitter offset was set at −479 749 Hz), and for complex **3** five subspectra spaced by 27.9 kHz (the first transmitter offset was set at −454 676 Hz). In all cases, the subspectra were coadded using the skyline projection method. The acquisition time ($1/\tau_a$) was adjusted to attain a spikelet separation of 8.3 kHz for complex **1**, 4.3 kHz for complex **2**, and 3.1 kHz for complex **3**. ^{1}H−^{195}Pt CP/CPMG (Carr−Purcell Meiboom−Gill) experiments were performed using a 3.25 μs proton $\pi/2$ pulse length, a ν_{CP} of 65.4 kHz, a contact time of 7.0 ms, a ν_{dec} of 77.0 kHz, and a recycle delay of 4 s. ^{19}F MAS NMR experiments were performed using the Bloch decay pulse sequence with a $\pi/2$ fluorine pulse length of 3 μs and a recycle delay of 6 s. The spinning rates for ^{1}H−^{31}P CP/MAS (and ^{19}F MAS) NMR spectra were chosen in such a way that the second-order effects were completely averaged.[38] The ^{1}H−^{31}P CP/MAS NMR spectrum of **3** recorded at a spinning rate of 9.0 kHz showed too few spinning sidebands, precluding a suitable HB analysis.[39] Therefore, the spectrum was recorded also at a 4.0 kHz spinning rate, which was a good compromise between the need to average second-order effects[38] and the need to generate at least five intense spinning sidebands for HB analysis.

Simulations of static spectra were carried out with WSOLIDS,[40] while simulation of MAS spectra was carried out with SIMPSON.[41] The shown calculated solid-state ^{31}P NMR spectra were obtained as addition of three subspectra of isotopomers having no (natural abundance: 43.8%), one (natural abundance: 44.8%), or two (natural abundance: 11.4%) NMR-active ^{195}Pt atoms. The HB analysis was performed using the program Graphical Herzfeld Berger Analysis.[42]

COMPUTATIONAL DETAILS

All calculations have been carried out using density functional theory (DFT) as implemented in the Amsterdam Density Functional (ADF 2013) code.[43] Relativistic effects were modeled by the two-component zero-order regular approximation (ZORA) method,[29] including either only scalar effects (ZSC) or spin−orbit coupling (ZSO) as well. In keeping with previous studies,[44,45] we adopted the BP86 functional[46,47] and basis sets made of triple-ζ quality, singly or doubly polarized Slater functions (TZP and TZ2P, respectively). Geometry optimization was performed at the ZSC/TZP level under C_i (**1** and **2**) or C_2 (**3**) symmetry, and the calculation of molecular properties at the ZSO/TZ2P level (without symmetry constraints).

NMR properties of ^{195}Pt and ^{31}P nuclei were calculated with the ADF NMR module[48−51] from the ZSO density and yielded the full shielding tensor and its principal components σ_{11}, σ_{22}, and σ_{33}, with $\sigma_{33} \geq \sigma_{22} \geq \sigma_{11}$. Chemical shifts were determined as $\delta_{ii} = (\sigma_{ref} - \sigma_{ii})/(1 - \sigma_{ref})$ using the commonly adopted reference $[PtCl_6]^{2-}$ (σ_{ref} = 1397.9 ppm)[45] for ^{195}Pt and as $\delta_{ii} = (\sigma_{ref} - \sigma_{ii} - 266.1)$[52] relative to 85% H_3PO_4 using the magnetic shielding constant of PH_3 (σ_{ref} = 589.8 ppm) calculated at the same computational level as the secondary reference.

Chemical shift anisotropies were obtained as $\Omega = \delta_{11} - \delta_{33}$ and $\kappa = 3(\delta_{22} - \delta_{iso})/\Omega$. ^{195}Pt chemical shifts were calibrated against a set of Pt(II) and Pt(IV) complexes spanning the range between −6000 and 7000 ppm, obtained at the same theoretical level.[45]

RESULTS AND DISCUSSION

^{1}H−^{31}P CP/MAS NMR. The solution ^{31}P{^{1}H} NMR spectra of the compounds depicted in Chart 3 exhibit one signal for the two equivalent ^{31}P nuclei at δ −147 for **1**;[34] δ 282 for **2**;[35] and δ −8 for **3**[34] flanked by ^{195}Pt satellites (for **1**: $^1J_{P,Pt}$ = 1787 Hz; for **2**: $^1J_{P,Pt}$ = 1224 Hz; for **3**: $^1J_{P,Pt}$ = 2175 Hz). In the solid state, ^{1}H−^{31}P CP/MAS NMR spectra of the dinuclear complexes **1**

DOI: 10.1021/acs.inorgchem.5b00627
Inorg. Chem. 2015, 54, 5855−5863

and **2** (Figures 1 and 2) exhibited a single spinning sideband pattern compatible with a crystallographic equivalence of both

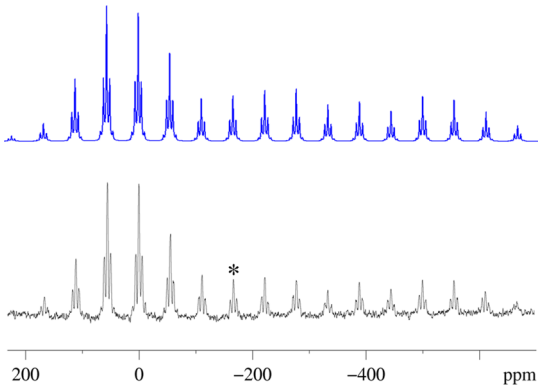

Figure 1. $^{1}H-^{31}P$ CP/MAS spectrum of $(nBu_4N)_2[(C_6F_5)_2Pt(\mu\text{-}PPh_2)_2Pt(C_6F_5)_2]$, **1**, obtained with a MAS rate of 9.0 kHz, a 6.0 s recycle delay (bottom trace), and spectral simulation using the data listed in Table 1 (top trace). The asterisk indicates the isotropic ^{31}P chemical shift.

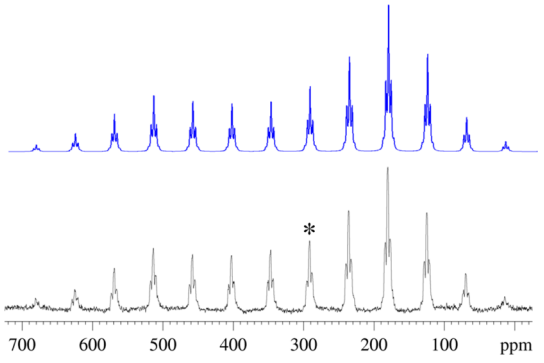

Figure 2. $^{1}H-^{31}P$ CP/MAS spectrum of $[(C_6F_5)_2Pt(\mu\text{-}PPh_2)_2Pt\text{-}(C_6F_5)_2]$(*Pt–Pt*), **2**, obtained with a MAS rate of 9.0 kHz (bottom trace) and spectral simulation using the data listed in Table 1 (top trace). The asterisk indicates the isotropic ^{31}P chemical shift.

^{31}P nuclei,[53] while the spectrum of **3** (Figure 3) showed two different signals with equal intensities, in accord with the presence of two crystallographically inequivalent phosphorus nuclei within the molecule.[54] The presence of two crystallographically inequivalent phosphorus nuclei in *cis*-$Pt(PR_3)_2X_2$ complexes is unexceptional, as it has been noted that usually the crystal symmetry for the two phosphine ligands of one complex renders each phosphorus crystallographically distinct.[35,55,56]

In the case of **1** and **2**, the isotropic $^{1}H-^{31}P$ CP/MAS chemical shifts are δ −166 and 292, respectively, with indirect coupling constants $^{1}J_{P,Pt}$ = 1775 (**1**) and $^{1}J_{P,Pt}$ = 1220 Hz (**2**). For **3**, the isotropic $^{1}H-^{31}P$ CP/MAS chemical shifts are δ −4 and δ −7, with a $^{1}J_{P,Pt}$ of 2175 and 2120 Hz, respectively. The relatively good agreement with the solution shifts indicates the absence of significant structural differences between solid state and solution.

The principal components of the ^{31}P chemical shift tensors obtained from Herzfeld–Berger (HB) analysis of the sideband patterns[57] of complexes **1**, **2**, and **3** are collected in Table 1. For both diphenylphosphanido-bridged complexes **1** and **2**, the chemical shieldings of the ^{31}P nucleus exhibit considerable anisotropy, as measured by the span Ω of the chemical shift

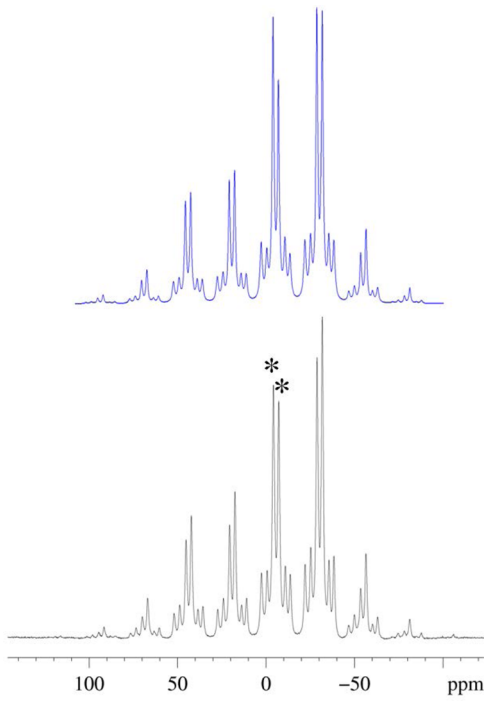

Figure 3. $^{1}H-^{31}P$ CP/MAS spectrum of *cis*-$Pt(C_6F_5)_2(PHPh_2)_2$, **3**, obtained with a MAS rate of 4.0 kHz (bottom trace) and spectral simulation using the data listed in Table 1 (top trace). The asterisks indicate the isotropic ^{31}P chemical shifts of the inequivalent P atoms.

(CS) tensor, which is 840 ppm for **1** and 595 ppm for **2**. Such values are comparable with that obtained for μ-PHMes in the Pt dimer *anti*-$[(PH_2Mes)ClPt(\mu\text{-}PHMes)Pt(PH_2Mes)Cl]$ (Ω = 712 ppm).[58,59] As a comparison, diphenylphosphanido-bridged Fe, Ru, or Os complexes show spans ranging from 206 to 620 ppm,[60] the latter value being observed for the cluster $Ru_8(CO)_{21}(\mu_6\text{-}P)(\mu_4\text{-}PPh)(\mu_2\text{-}PPh_2)$. However, closer inspection of the three tensor components of **1** and **2** (and of the corresponding skews) reveals that the high anisotropies arise primarily from a large offset of a single principal component, whereas the other two components remain almost unchanged and are quite similar in both complexes. In fact, for **1** the distinct principal component is δ_{33}, with a value of −698 ppm, responsible for the high-field frequency of the ^{31}P isotropic signal and the positive sign of the skew (κ = 0.80), while for **2** the distinct principal component is δ_{11}, with a value of 649 ppm, responsible for the low-field frequency of the ^{31}P isotropic signal (and the negative sign of the skew, κ = −0.60). The other two tensor components of the bridging phosphanides have values of 142 and 59 ppm for **1** and 172 and 54 ppm for **2**.

As a consequence of the local symmetry around phosphorus, we may assume that two of the three tensor components lie approximately in the coordination plane of platinum, and the third one is nearly perpendicular to it. By analogous reasoning to that used by Lindner for cyclic biphosphane complexes of Mo, W, and Pt,[61] we assign in both complexes the *distinct* principal component (δ_{33} in case of **1** and δ_{11} in case of **2**) as the one that is oriented perpendicular to the Pt_2P_2 plane.[62] This hypothesis was confirmed by DFT calculations (*vide infra*). Consequently, the higher $\delta_{iso^{31}P}$ of **2** in comparison to **1** is exclusively attributable to a large variation of the shielding (by some 1350 ppm) along the axis perpendicular to the Pt coordination planes.

DOI: 10.1021/acs.inorgchem.5b00627
Inorg. Chem. 2015, 54, 5855−5863

Table 1. Experimental Solid-State and Solution ^{31}P Parameters of 1−3

complex	ν_{rot} (kHz)	δ_{11} (ppm)	δ_{22} (ppm)	δ_{33} (ppm)	δ_{iso} (ppm)[a]	$^{1}J_{P,Pt}$ (Hz)	Ω (ppm)[b]	κ[c]	$\delta_{solution}$ (ppm)
1	9.0	142(11)	59(8)	−698(8)	−166	1775	840 (6)	0.80 (0.8)	−147[d]
2	9.0	649(2)	172(1)	54(1)	292	1220	595 (2)	−0.60 (0.01)	282[d]
3	4.0	65(1)	−31(1)	−47(1)	−4	2175	112 (0.2)	−0.72 (0.01)	−7.8[e]
		70(1)	−28(1)	−64(1)	−7	2120	134 (0.2)	−0.47 (0.01)	

[a]Isotropic shift is defined as $\delta_{iso} = (\delta_{11} + \delta_{22} + \delta_{33})/3$. [b]$\Omega = \delta_{11} - \delta_{33}$. [c]$\kappa = 3(\delta_{22} - \delta_{iso})/\Omega$. [d]From ref 35. [e]From ref 34.

In the mononuclear complex **3**, where the diphenylphosphane ligands are terminally bonded to Pt, the spans of the ^{31}P shielding tensors (Ω = 112 and 134 ppm) are much smaller than in **1** or **2**, falling in the range of those reported for phosphanes terminally coordinated to platinum.[55,56,61]

^{1}H−^{195}Pt CP/CPMG NMR. Differently from the solution-state case, where ^{195}Pt NMR is now an established analytical tool for characterizing platinum-containing molecules, solid-state ^{195}Pt NMR studies are still rare.[37,56,63−78] The difficulties in recording high-resolution solid-state ^{195}Pt NMR spectra are largely due to the exceedingly high chemical shift anisotropy (in some cases higher than 10 000 ppm)[59] exhibited by this nucleus in a square planar coordination geometry, resulting in extremely broad patterns with correspondingly low signal-to-noise (S/N) ratios. When the platinum nucleus is coupled with several NMR-active nuclei, the task of recording clear MAS ^{195}Pt NMR spectra is even more challenging, due to multiple direct, indirect, and quadrupolar couplings. An elegant solution, proposed independently by Wasylishen[37] and Schurko,[36] consists in the application of the Carr−Purcell Meiboom−Gill pulse sequence for the acquisition of static solid-state NMR of spin-1/2 nuclei with a good S/N ratio in reasonable acquisition times. The FID of CPMG experiments contains a series of echoes that, after Fourier transformation, result in a manifold of "spikelets" in the frequency domain. The envelope of these "spikelets", in the case of a spin-1/2 nucleus such as ^{195}Pt, allows the reconstruction of the shape of the static powder pattern. A drawback of the use of the CPMG pulse sequence is the loss of signal multiplicity, which, in the present study, is irrelevant. CPMG and CP/CPMG pulse sequences have been applied to the solid-state NMR study of $[Pt(PPh_3)_2(C_2H_4)]$,[37] $[Pt(PEt_3)_2(OCO)_2{\cdot}xH_2O]$,[37] $Pt[S_2C_2(CF_3)_2]_2$[79] and its reduced form,[80] Pt(II) complexes with hexadentate amino- and iminophosphane ligands,[81] and $[Pt(dbbpy)(C{\equiv}CC_6H_4BMes_2)_2]$ (dbbpy = 4,4′-di-*tert*-butyl-2,2′-bipyridine).[74]

The static ^{1}H−^{195}Pt CP/CPMG spectra of complexes **1** and **2** are reported in Figure 4a,b. Analytical simulation of the static powder pattern envelope furnished δ_{iso} −3767 for **1** and δ_{iso} −5389 for **2**, values in reasonable accord with those obtained in acetone-d_6 solution (Table 2). The span observed for **1** (Ω = 4549 ppm) is comparable to that found for $[Pt(dbbpy)(C{\equiv}CC_6H_4BMes_2)_2]$ (Ω = 4150 ppm)[74] and much larger than one might expect on the basis of the literature. In fact, pioneering works on ^{1}H−^{195}Pt CP/MAS suggested that, independently of the formal oxidation state of platinum, the span found for complexes endowed with the *cis*-P_2PtC_2[56] fragment should be modest (500−1300 ppm).[66]

In the case of **1**, the large chemical shift anisotropy (CSA) arises mainly from large deshielding in the direction of δ_{11}, which was estimated as high as −1023 ppm, with respect to the other two components (δ_{22} −4705 ppm, δ_{33} −5572 ppm). As far as **2** is concerned, it can be observed that two principal components of the ^{195}Pt shift tensor (δ_{11} at −4618 ppm and δ_{22} at −5594 ppm) are quite similar to δ_{22} and δ_{33} of **1**, while the third one, which is the most shielded component (δ_{33} −5954 ppm) is very different from δ_{11} of **1**. Again, local symmetry arguments suggest that the principal components, for both **1** and **2**, are oriented one perpendicular and two in-plane with respect to the coordination plane. Given the similarity to the ^{31}P case, we may assume that the principal components of the ^{195}Pt shift tensor, which have similar magnitudes in **1** and in **2** (δ_{22} and δ_{33} for **1** and δ_{11} and δ_{22} for **2**), are oriented in-plane, while the remaining principal component (δ_{11} for **1** and δ_{33} for **2**) is perpendicular to the coordination plane. This hypothesis is, again, supported by the DFT calculations[82] (*vide infra*).

The large shielding difference (ca. 5000 ppm) observed comparing δ_{11} of **1** to δ_{33} of **2** (the two other principal components being almost the same) causes a dramatic reduction of CSA, attested by a tensor span for **2** of 1337 ppm.

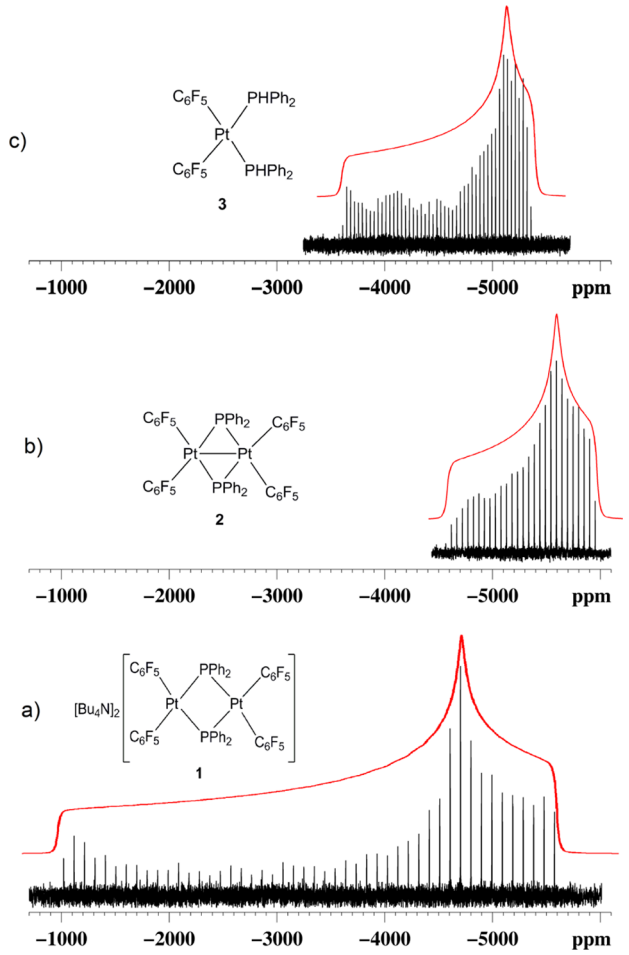

Figure 4. Static ^{1}H−^{195}Pt CP/CPMG spectra (bottom trace) and simulations of powder patterns (top trace in red) of **1** (a), **2** (b), and **3** (c).

DOI: 10.1021/acs.inorgchem.5b00627
Inorg. Chem. 2015, 54, 5855−5863

Table 2. Experimental Solid-State and Solution ^{195}Pt Parameters of 1−3

complex	δ_{11} (ppm)	δ_{22} (ppm)	δ_{33} (ppm)	δ_{iso} (ppm)[a]	Ω (ppm)[b]	κ[c]	$\delta_{solution}$ (ppm)
1	−1023(48)	−4705(48)	−5572(48)	−3767(83)	4549(67)	−0.62(2)	−3795[d]
2	−4618(26)	−5594(26)	−5954(26)	−5389(45)	1337(36)	−0.46(3)	−5298
3	−3613(18)	−5104(18)	−5359(18)	−4692(31)	1747(25)	−0.71(3)	−4677

[a]Isotropic shift is defined as $\delta_{iso} = (\delta_{11} + \delta_{22} + \delta_{33})/3$. [b]$\Omega = \delta_{11} - \delta_{33}$. [c]$\kappa = 3(\delta_{22} - \delta_{iso})/\Omega$. [d]In acetone-$d_6$, from ref 2.

Table 3. Detailed ^{31}P and ^{195}Pt Isotropic Shieldings in 1−3

	σ_p	σ_d	σ_{SO}	σ_{iso}	δ_{iso}
^{31}P					
$[(C_6F_5)_2Pt(\mu\text{-}PPh_2)_2Pt(C_6F_5)_2]^{2-}$ (**1**)	−639.5	962.2	127.9	450.6	−126.9
$[(C_6F_5)_2Pt(\mu\text{-}PPh_2)_2Pt(C_6F_5)_2]$*(Pt−Pt)* (**2**)	−922.7	963.2	−1.52	38.9	284.8
cis-$[Pt(C_6F_5)_2(PHPh_2)_2]$ (**3**) P1	−682.7	963.0	30.1	310.3	13.4
cis-$[Pt(C_6F_5)_2(PHPh_2)_2]$ (**3**) P2	−682.6	963.0	30.1	310.5	13.2
^{195}Pt					
$[(C_6F_5)_2Pt(\mu\text{-}PPh_2)_2Pt(C_6F_5)_2]^{2-}$ (**1**)	−7330.7	9281.9	2641.3	4592.5	−3199.1
$[(C_6F_5)_2Pt(\mu\text{-}PPh_2)_2Pt(C_6F_5)_2]$*(Pt−Pt)* (**2**)	−6000.6	9282.7	2670.4	5952.5	−4561.0
cis-$[Pt(C_6F_5)_2(PHPh_2)_2]$ (**3**)	−6349.2	9587.2	2839.4	6077.4	−4686.0

Comparing the ^{31}P and ^{195}Pt data of **1** and **2** it is apparent that, while the ^{195}Pt nuclei of **1** are more deshielded than those of **2**, the ^{31}P nuclei of **1** are more shielded than those of **2**. This behavior has been already noticed for platinum complexes bearing chelating diphosphanes forming four- to six-membered rings.[61]

The isotropic ^{195}Pt chemical shift of **3** was determined as −4692 ppm, in accord with the value observed in chloroform solution (δ −4677). For **3**, whose ^{1}H−^{195}Pt CP/CPMG spectrum is reported in Figure 4c, the tensor span (Ω 1747 ppm) is comparable to that of mononuclear Pt complexes with a *cis*-P_2PtC_2 fragment.[38] This points out that the large CSA observed for **1** should be ascribed to the presence of the four-membered P_2Pt_2 ring present in **1** but not in **3**.

DFT Calculation of ^{31}P and ^{195}Pt Chemical Shielding Tensor Parameters. Theoretical calculations of ^{31}P and ^{195}Pt CS tensors were performed to confirm the tensor orientation proposed from experimental data and symmetry arguments. ^{31}P and ^{195}Pt and shielding tensors were computed with relativistic DFT methods including spin−orbit coupling (see Computational Details).

Isotropic Chemical Shifts: ^{31}P. Experimental ^{31}P isotropic shifts in solution are δ −147 (**1**), 282 (**2**), and −7.8 ppm (**3**); the corresponding calculated shifts are δ −127, 285, and 13 ppm, respectively. While the absolute shifts are somewhat different, the shift difference $\Delta\delta_{calc}$(**1**−**2**) = 413 ppm matches the experimental one ($\Delta\delta_{exp}$ = 429 ppm). The two P atoms in **3** differ only slightly in their NMR properties and are observed as a single signal in solution; the calculated shifts indeed differ by just 0.15 ppm.

A point of interest concerns spin−orbit effects on the relative shielding of ^{31}P in **1** and **2** (the electronic structure of **3** is too different to warrant this analysis). Table 3 shows that the different values of σ_{iso} stem from differences in both σ_p and σ_{SO} (σ_d being almost constant, as expected). In particular, σ_{SO} (128 ppm) is positive and of sizable magnitude for **1**, whereas it is almost zero for **2**. Relativistic effects on the shielding of a light atom bonded to a heavy one are well-known, especially on ^{13}C bonded to heavy halogens,[83,84] and have been traced to the *s*-character of the bond between the two atoms. Moreover, the sign of σ_{SO} has been related to the bond type, a positive value being associated with high-energy occupied MOs with local π character.[85,86] Analysis of high-energy MOs of **1** and **2** highlights that in the case of **1** the MO mostly accounting for the Pt−P bond has a high π character. Conversely, the Pt−P bond in **2** is described by a σ-type MO (Figure 5). On the other hand, the HOMO−LUMO gaps (0.110 and 0.063 au for **1** and **2**, respectively), which are often surmised to be an important factor affecting both σ_p and σ_{SO},[87] follow the expected trend regarding σ_p but do not seem to play a major role for σ_{SO}. Other analyses based on natural localized, rather than canonical, orbitals[88,89] are hampered by the large size of **1** and **2**.

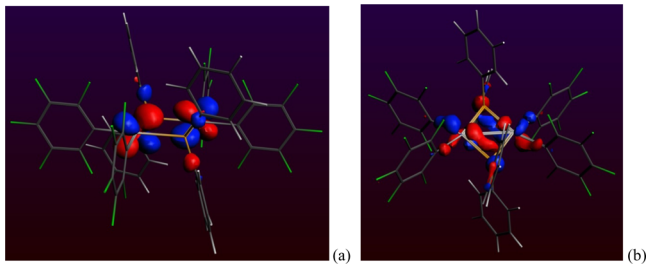

Figure 5. (a) MO #162 (A_u symmetry) of **1**; (b) MO #158 (A_u symmetry) of **2**.

Isotropic Chemical Shifts: ^{195}Pt. The accuracy of predicted shieldings was first assessed by correlating experimental and calculated isotropic shifts for a variety of Pt(II) and Pt(IV) complexes for which experimental data are available (Table S1).[45] Literature values for known mononuclear complexes are very well correlated; least-squares fitting ($\delta_{calc} = b\delta_{exp} + a$) yields b = 0.94, a = 155 ppm, R^2 = 0.98 (Figure S4). Apart from the systematic offset of 155 ppm (commonly encountered in these correlations),[45,90] calculated shifts are underestimated by 6%. The shieldings for $[(C_6F_5)_2Pt(\mu\text{-}PPh_2)_2Pt(C_6F_5)_2]^{2-}$ (**1**), $[(C_6F_5)_2Pt(\mu\text{-}PPh_2)_2Pt(C_6F_5)_2]$*(Pt−Pt)* (**2**), and *cis*-$[Pt(PHPh_2)_2(C_6F_5)_2]$ (**3**) (red markers in Figure S4) fully fit the correlation. Therefore, the results indicate that the theoretical method adopted is reliable.

Shielding Tensors and Anisotropies. The principal components of the ^{31}P and ^{195}Pt shielding tensors, shifts, and anisotropies are reported in Table 4; principal components are

DOI: 10.1021/acs.inorgchem.5b00627
Inorg. Chem. 2015, 54, 5855−5863

Table 4. Principal Components and Anisotropies of the ^{31}P and ^{195}Pt Shielding Tensors of 1−3[a]

	σ_{11}	σ_{22}	σ_{33}	δ_{11}	δ_{22}	δ_{33}	Ω	κ
^{31}P								
$[(C_6F_5)_2Pt(\mu\text{-}PPh_2)_2Pt(C_6F_5)_2]^{2-}$ (**1**)	168.1	251.8	931.9	156	72	−608	764	0.78
$[(C_6F_5)_2Pt(\mu\text{-}PPh_2)_2Pt(C_6F_5)_2]$ (**2**)	−266.8	126.2	257.4	591	197	66	524	−0.50
cis-$[Pt(C_6F_5)_2(PHPh_2)_2]$ (**3**) P1	245.9	336.3	348.8	78	−13	−25	103	−0.76
cis-$[Pt(C_6F_5)_2(PHPh_2)_2]$ (**3**) P2	245.9	336.6	349.0	78	−13	−25	103	−0.76
^{195}Pt								
$[(C_6F_5)_2Pt(\mu\text{-}PPh_2)_2Pt(C_6F_5)_2]^{2-}$ (**1**)	2089.3	5392.6	6295.6	−693	−4000	−4905	4212	−0.57
$[(C_6F_5)_2Pt(\mu\text{-}PPh_2)_2Pt(C_6F_5)_2]$ (**2**)	4975.2	6291.0	6591.4	−3582	−4900	−5201	1618	−0.63
cis-$[Pt(C_6F_5)_2(PHPh_2)_2]$ (**3**)	5222.0	6402.1	6608.0	−3829	−5011	−5217	1388	−0.70

[a]In ppm at the ZSO-BP86/TZ2P level (see text).

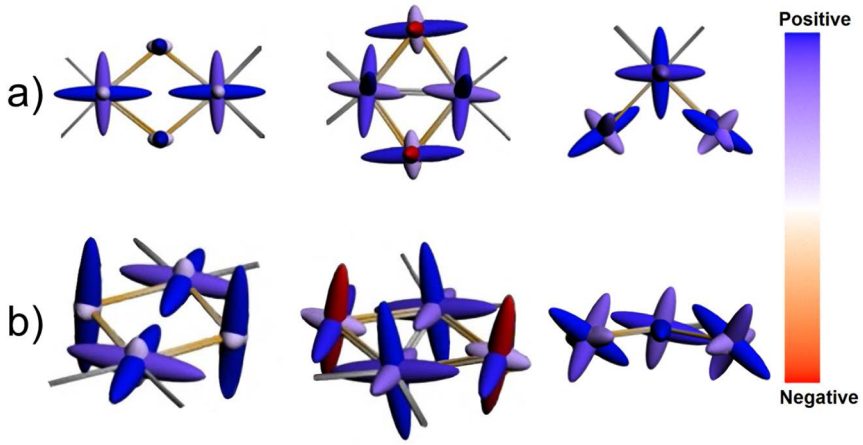

Figure 6. Orientation of the principal components of the shielding tensors of ^{195}Pt and ^{31}P in $[(C_6F_5)_2Pt(\mu\text{-}PPh_2)_2Pt(C_6F_5)_2]^{2-}$ (**1**) (left), $[(C_6F_5)_2Pt(\mu\text{-}PPh_2)_2Pt(C_6F_5)_2]_{(Pt-Pt)}$ (**2**) (middle), and *cis*-$[Pt(C_6F_5)_2(PHPh_2)_2]$ (**3**) (right). (a) Top view, (b) side view. Positive and negative shielding values are encoded according to the color map on the right. Phenyl and C_6F_5 rings are omitted for clarity.

plotted against the molecular structures in Figure 6. Detailed values of the individual tensor components and plots for **1**−**3** are provided in the Supporting Information (Tables S2−S4) and plotted against the molecular framework (Figures S5−S10). These data show that for Pt the largest (most shielded) principal components are in the coordination plane for **1** but perpendicular to it for **2**. Analysis of individual contributions for **1** and **2** indicates that while the diamagnetic and (to a minor extent) spin−orbit terms affect the overall magnitude of the shielding tensor σ, its orientation for both ^{195}Pt and ^{31}P is essentially that of σ_p. Moreover, the small ^{195}Pt component perpendicular to the coordination plane of **1** is seen to arise from a partial cancellation of the respective diamagnetic and paramagnetic terms (Figure S5); a similar cancellation occurs also for **2**, but to a lesser extent (Figure S7). For **3**, the orientation derives from all tensor components.

CONCLUSIONS

This work highlights the influences contributing to the ^{31}P and ^{195}Pt chemical shifts for diphenylphosphanido-bridged diplatinum compounds. Combined solid-state NMR and DFT calculations on complexes indicate that the distinct principal components of the chemical shift tensors of $(nBu_4N)_2[(C_6F_5)_2Pt(\mu\text{-}PPh_2)_2Pt(C_6F_5)_2]$ (**1**) and $[(C_6F_5)_2Pt(\mu\text{-}PPh_2)_2Pt(C_6F_5)_2](Pt-Pt)$ (**2**) are oriented in both cases along the direction perpendicular to the Pt_2P_2 plane. However, while ^{31}P nuclei of **2**, with respect to **1**, are significantly *deshielded* (by ca. 1350 ppm) along the direction of the distinct principal component of the CS tensor, ^{195}Pt nuclei of **2**, compared to **1**, are strongly *shielded* (by ca. 5000 ppm) along the directions of the distinct principal component of the CS tensor. DFT calculations showed that the different values of σ_{iso} stem, for ^{31}P, from differences in the paramagnetic (σ_p) and in the spin−orbit term (σ_{SO}), and for ^{195}Pt, from differences mainly in σ_p.

ASSOCIATED CONTENT

Supporting Information

Details of the ^{195}Pt and ^{31}P shielding tensors, ^{19}F MAS spectra and parameters with discussion, orientation of the principal individual components of the shielding tensors of ^{195}Pt and ^{31}P, Cartesian coordinates at the BP86-ZORA-SC/TZP level of complexes **1**−**3**. The Supporting Information is available free of charge on the ACS Publications website at DOI: 10.1021/acs.inorgchem.5b00627.

AUTHOR INFORMATION

Corresponding Author

*E-mail: p.mastrorilli@poliba.it. Fax: +39 080 5963611. Tel: +39 080 5963666.

Notes

The authors declare no competing financial interest.

[¶]Deceased on March 24, 2015.

ACKNOWLEDGMENTS

Prof. Juan Foniés (University of Zaragoza) is gratefully acknowledged for exciting discussions on platinum phosphanido complexes. We thank Dr. Giacomo Saielli for kind help in

DOI: 10.1021/acs.inorgchem.5b00627
Inorg. Chem. 2015, 54, 5855−5863

some DFT calculations. The Politecnico di Bari, the University of Padua, the University of Stuttgart, the Spanish MINECO/FEDER (Project No. CTQ2012-35251), and the Gobierno de Aragón (Grupo Consolidado E21: Química Inorgánica y de los Compuestos Organometálicos) are gratefully acknowledged for financial support.

REFERENCES

(1) Mastrorilli, P. *Eur. J. Inorg. Chem.* **2008**, 4835−4850 and references therein.
(2) Ara, I.; Forniés, J.; Fortuño, C.; Ibáñez, S.; Martín, A.; Mastrorilli, P.; Gallo, V. *Inorg. Chem.* **2008**, *47*, 9069−9080.
(3) Fabrizi de Biani, F.; Manca, G.; Marchetti, L.; Leoni, P.; Bruzzone, S.; Guidotti, C.; Atrei, A.; Albinati, A.; Rizzato, S. *Inorg. Chem.* **2009**, *48*, 10126−10137.
(4) Alonso, E.; Forniés, J.; Fortuño, C.; Lledós, A.; Martín, A.; Nova, A. *Inorg. Chem.* **2009**, *48*, 7679−7690.
(5) Leary, E.; Van Zalinge, H.; Higgins, S. J.; Nichols, R. J.; Fabrizi de Biani, F.; Leoni, P.; Marchetti, L.; Zanello, P. *Phys. Chem. Chem. Phys.* **2009**, *11*, 5198−5202.
(6) Albinati, A.; Balzano, F.; Fabrizi de Biani, F.; Leoni, P.; Manca, G.; Marchetti, L.; Rizzato, S.; Uccello Barretta, G.; Zanello, P. *Inorg. Chem.* **2010**, *49*, 3714−3720.
(7) Mastrorilli, P.; Latronico, M.; Gallo, V.; Polini, F.; Re, N.; Marrone, A.; Gobetto, R.; Ellena, S. *J. Am. Chem. Soc.* **2010**, *132*, 4752−4765.
(8) Forniés, F.; Fortuño, C.; Ibáñez, S.; Martín, A.; Mastrorilli, P.; Gallo, V. *Inorg. Chem.* **2011**, *50*, 10798−10809.
(9) Latronico, M.; Mastrorilli, P.; Gallo, V.; Dell'Anna, M. M.; Creati, F.; Re, N.; Englert, U. *Inorg. Chem.* **2011**, *50*, 3539−3558.
(10) Forniés, J.; Fortuño, C.; Ibáñez, S.; Martín, A.; Romero, P.; Mastrorilli, P.; Gallo, V. *Inorg. Chem.* **2011**, *50*, 285−298.
(11) Arias, A.; Forniés, J.; Fortuño, C.; Martín, A.; Latronico, M.; Mastrorilli, P.; Todisco, S.; Gallo, V. *Inorg. Chem.* **2012**, *51*, 12682−12696.
(12) Latronico, M.; Sánchez, S.; Rizzuti, A.; Gallo, V.; Polini, F.; Lalinde, E.; Mastrorilli, P. *Dalton Trans.* **2013**, *42*, 2502−2511.
(13) Arias, A.; Forniés, F.; Fortuño, C.; Martín, A.; Mastrorilli, P.; Todisco, S.; Latronico, M.; Gallo, V. *Inorg. Chem.* **2013**, *52*, 5493−5506.
(14) Arias, A.; Forniés, F.; Fortuño, C.; Ibáñez, S.; Martín, A.; Mastrorilli, P.; Todisco, S.; Gallo, V. *Inorg. Chem.* **2013**, *52*, 11398−11408.
(15) Funaioli, T.; Leoni, P.; Marchetti, L.; Albinati, A.; Rizzato, S.; Fabrizi de Biani, F.; Ienco, A.; Manca, G.; Mealli, C. *Inorg. Chem.* **2013**, *52*, 4635−4647.
(16) Bonuccelli, V.; Funaioli, T.; Leoni, P.; Marchetti, P.; Marchetti, L. *Inorg. Chem.* **2013**, *52*, 8759−8769.
(17) Latronico, M.; Todisco, S.; Gallo, V.; Englert, U.; Mastrorilli, P. *Eur. J. Inorg. Chem.* **2014**, *10*, 1669−1678.
(18) Arias, A.; Forniés, J.; Fortuño, C.; Martín, A.; Mastrorilli, P.; Gallo, V.; Latronico, M.; Todisco, S. *Eur. J. Inorg. Chem.* **2014**, *10*, 1679−1693.
(19) Bender, R.; Welter, R.; Braunstein, P. *Inorg. Chim. Acta* **2015**, *424*, 20−28.
(20) Petersen, J. L.; Stewart, R. P., Jr. *Inorg. Chem.* **1980**, *19*, 186−191.
(21) Carty, A. J.; Hartstock, F.; Taylor, N. J. *Inorg. Chem.* **1982**, *21*, 1349−1354.
(22) Garrou, P. E. *Chem. Rev.* **1981**, *81*, 229−266.
(23) Pregosin, P. S. *Coord. Chem. Rev.* **1982**, *44*, 247−291.
(24) Pregosin, P. S. *Annu. Rep. NMR Spectrosc.* **1986**, *17*, 285−349.
(25) Still, B. M.; Kumar, P. G.; Aldrich Wright, J. R.; Price, W. S. *Chem. Soc. Rev.* **2007**, *36*, 665−686.
(26) Priqueler, J.R. L.; Butler, I. S.; Rochon, F. D. *Appl. Spectrosc. Rev.* **2006**, *41*, 185−226.
(27) In this class of compounds we have included the hydrido-phosphanido-bridged diplatinum complexes that can be considered protonated Pt(I) complexes. See: Gallo, V.; Latronico, M.; Mastrorilli, P.; Polini, F.; Re, N.; Englert, U. *Inorg. Chem.* **2008**, *47*, 4785−4795 and references therein.
(28) See for example: (a) Grutzner, J. B. In *Recent Advances in Organic NMR Spectroscopy*; Lambert, J. B.; Rittner, R., Eds.; Norell Press, 1987; Chapter 2, pp 17−42. (b) Kutzelnigg, W.; van Wüllen, C.; Fleischer, U.; Franke, R.; Mourik, T. In *Nuclear Magnetic Shielding and Molecular Structure*; Tossell, J. A., Ed.; NATO ASI Series C; Kluwer: Dordrecht, 1993; Vol. *386*, pp 141−161. (c) Bagno, A.; Bonchio, M. *Chem. Phys. Lett.* **2000**, *317*, 123−128.
(29) *Calculation of NMR and EPR Parameters: Theory and Applications*; Kaupp, M.; Bühl, M.; Malkin, V. G., Eds.; Wiley-VCH: Weinheim, 2004.
(30) Goodfellow, R. J. In *Multinuclear NMR*; Mason, J., Ed.; Plenum Press: New York, 1987; p 52.
(31) Gilbert, T. M.; Ziegler, T. *J. Phys. Chem. A* **1999**, *103*, 7535−7543.
(32) Carty, A. J.; MacLaughlin, S. A.; Nucciarone, D. In *Phosphorus-31 NMR Spectroscopy in Stereochemical Analysis: Organic Compounds and Metal Complexes*; Verkade, J. G., Quin, L. D., Eds.; VCH Publishers: New York, 1987; Chapter 16, and references therein.
(33) In this regard, being that magnetic shielding is a localized phenomenon, the nature of the orbitals about the nucleus of interest may also be important.
(34) Forniés, J.; Fortuño, C.; Navarro, R.; Martínez, F.; Welch, A. J. *J. Organomet. Chem.* **1990**, *394*, 643−658.
(35) Alonso, E.; Casas, J. M.; Cotton, F. A.; Feng, X.; Forniés, J.; Fortuño; Tomas, M. *Inorg. Chem.* **1999**, *38*, 5034−5040.
(36) Hung, I.; Rossini, A. J.; Schurko, R. W. *J. Phys. Chem. A* **2004**, *108*, 7112−7120.
(37) Siegel, R.; Nakashima, T. T.; Wasylishen, R. E. *J. Phys. Chem. B* **2004**, *108*, 2218−2226.
(38) Challoner, R.; Sebald, A. *Solid State Nucl. Magn. Reson.* **1995**, *4*, 39−45.
(39) Hodgkinson, P.; Emsley, L. *J. Chem. Phys.* **1997**, *107*, 4808−4816.
(40) Eichele, K.; Wasylishen, R. E. *WSolids1*, ver. 1.20.21; Universität Tübingen, 2013.
(41) Bak, M.; Rasmussen, J. T.; Nielsen, N. C. *J. Magn. Reson.* **2000**, *147*, 296.
(42) Eichele, K. *HBA 1.7*; Universität Tübingen, 2012.
(43) te Velde, G.; Bickelhaupt, F. M.; Baerends, E. J.; Fonseca Guerra, C.; Van Gisbergen, S. J. A.; Snijders, J. G.; Ziegler, T. *J. Comput. Chem.* **2001**, *22*, 931−967.
(44) Bagno, A.; Bonchio, M.; Autschbach, J. *Chem.—Eur. J.* **2006**, *12*, 8460−8471.
(45) Bagno, A.; Bini, R. *Angew. Chem., Int. Ed.* **2010**, *49*, 1083−1086.
(46) Becke, A. D. *Phys. Rev. A* **1988**, *38*, 3098−3100.
(47) Perdew, J. P. *Phys. Rev. B* **1986**, *33*, 8822−8824.
(48) Schreckenbach, G.; Ziegler, T. *J. Phys. Chem.* **1995**, *99*, 606−611.
(49) Schreckenbach, G.; Ziegler, T. *Int. J. Quantum Chem.* **1997**, *61*, 899−918.
(50) Wolff, S. K.; Ziegler, T. *J. Chem. Phys.* **1998**, *109*, 895−905.
(51) Wolff, S. K.; Ziegler, T.; van Lenthe, E.; Baerends, E. J. *J. Chem. Phys.* **1999**, *110*, 7689−7698.
(52) van Wüllen, C. *Phys. Chem. Chem. Phys.* **2000**, *2*, 2137−2144.
(53) The equivalence of the two P atoms in **1** and **2** is in accord with the XRD structures of $[PEtPh_3]_2[(C_6F_5)_2Pt(\mu\text{-}PPh_2)_2Pt(C_6F_5)_2]$ and of **2** that have shown the presence of an inversion center in both cases (see ref 35).
(54) Kakeya, M.; Tanabe, M.; Nakamura, Y.; Osakada, K. *J. Organomet. Chem.* **2009**, *694*, 2270−2278.
(55) Power, W. P.; Wasylishen, R. E. *Inorg. Chem.* **1992**, *31*, 2176−2183.
(56) Harris, R. K.; McNaught, I. J.; Reams, P. *Magn. Reson. Chem.* **1991**, *29*, S60−S72.
(57) Herzfeld, J.; Berger, A. E. *J. Chem. Phys.* **1980**, *73*, 6021−6030.

DOI: 10.1021/acs.inorgchem.5b00627
Inorg. Chem. 2015, 54, 5855−5863

(58) Kourkine, I. V.; Chapman, M. B.; Glueck, D. S.; Eichele, K.; Wasylishen, R. E.; Yap, G. Y. A.; Liable-Sands, L. M.; Rheingold, A. L. *Inorg. Chem.* **1996**, *35*, 1478−1485.
(59) Eichele, K.; Wasylishen, R. E.; Corrigan, J. F.; Taylor, N. J.; Carty, A. J.; Feindel, K. W.; Bernard, G. M. *J. Am. Chem. Soc.* **2002**, *124*, 1541−1552.
(60) Carty, A. J.; Fyfe, C. A.; Lettinga, M.; Johnson, S.; Randall, L. H. *Inorg. Chem.* **1989**, *28*, 4120−4124.
(61) Lindner, E.; Fawzi, R.; Mayer, H. A.; Eichele, K.; Hiller, W. *Organometallics* **1992**, *11*, 1033−1043.
(62) The orientation of the principal components of the chemical shift tensor has been studied experimentally for diphenylphosphanido groups spanning ruthenium−ruthenium bonds. See ref 59.
(63) Sparks, S. W.; Ellis, P. D. *J. Am. Chem. Soc.* **1986**, *108*, 3215−3218.
(64) Harris, R. K.; Reams, P.; Packer, K. J. *J. Chem. Soc., Dalton Trans.* **1986**, 1015−1020.
(65) Duer, M. J.; Khan, M. S.; Kakkar, A. K. *Solid State Nucl. Magn. Reson.* **1992**, *1*, 13−16.
(66) Austin, E. J. W.; Barrie, P. J.; Clark, R. J. H. *J. Chem. Soc., Chem. Commun.* **1993**, 1404−1405.
(67) Ambrosius, F.; Klaus, E.; Schalle, T.; Sebald, A. *Z. Naturforsch. A* **1995**, *50a*, 423−428.
(68) Siegel, R.; Nakashima, T. T.; Wasylishen, R. E. *J. Phys. Chem. B* **2004**, *108*, 2218−2226.
(69) Grykalowska, A.; Nowak, B. *Solid State Nucl. Magn. Reson.* **2005**, *27*, 223−227.
(70) Kogut, E.; Tang, J. A.; Lough, A. J.; Widdifield, C. M.; Schurko, R. W.; Fekl, U. *Inorg. Chem.* **2006**, *45*, 8850−8852.
(71) Demko, B. A.; Wasylishen, R. E. *Inorg. Chem.* **2008**, *47*, 2786−2797.
(72) Rodina, T. A.; Lutsenko, I. A.; Gerasimenko, A. V.; Ivanov, A. V. *Russ. J. Coord. Chem.* **2009**, *35*, 534−540.
(73) Thibault, M.-H.; Lucier, B. E. G.; Schurko, R. W.; Fontaine, F.-G. *Dalton Trans.* **2009**, 7701−7716.
(74) Tang, J. A.; Kogut, E.; Norton, D.; Lough, A. J.; McGarvey, B. R.; Fekl, U.; Schurko, R. W. *J. Phys. Chem. B* **2009**, *113*, 3298−3313.
(75) Hudson, Z. M.; Sun, C.; Harris, K. J.; Lucier, B. E. G.; Schurko, R. W.; Wang, S. N. *Inorg. Chem.* **2011**, *50*, 3447−3457.
(76) Lucier, B. E. G.; Reidel, A. R.; Schurko, R. W. *Can. J. Chem.* **2011**, *89*, 919−937.
(77) Harris, K. J.; Lupulescu, A.; Lucier, B. E. G.; Frydman, L.; Schurko, R. W. *J. Magn. Reson.* **2012**, *224*, 38−47.
(78) Lucier, B. E. G.; Johnston, K. E.; Xu, W.; Hanson, J. C.; Senanayake, S. D.; Yao, S.; Bourassa, M. W.; Srebro, M.; Autschbach, J.; Schurko, R. W. *J. Am. Chem. Soc.* **2014**, *136*, 1333−1351.
(79) Kogut, E.; Tang, J. A.; Lough, A. J.; Widdifield, C. M.; Schurko, R. W.; Fekl, U. *Inorg. Chem.* **2006**, *45*, 8850−8852.
(80) Tang, J. A.; Kogut, E.; Norton, D.; Lough, A. J.; McGarvey, B. R.; Fekl, U.; Schurko, R. W. *J. Phys. Chem. B* **2009**, *113*, 3298−3313.
(81) Thibault, M.-H.; Lucier, B. E. G.; Schurko, R. W.; Fontaine, F.-G. *Dalton Trans.* **2009**, 7701−7716.
(82) It should be noted that the implications of these arguments remain unchanged even when the assignment of the rather similar values of δ_{22} and δ_{33} for **2** is reversed.
(83) Malkin, V. G.; Malkina, O. L.; Salahub, D. R. *Chem. Phys. Lett.* **1996**, *261*, 335−345.
(84) Kaupp, M.; Malkina, O. L.; Malkin, V. G.; Pyykkö, P. *Chem.—Eur. J.* **1998**, *4*, 118−126.
(85) Hrobárik, P.; Hrobáriková, V.; Greif, A. H.; Kaupp, M. *Angew. Chem., Int. Ed.* **2012**, *51*, 10884−10888.
(86) Seaman, L. A.; Hrobárik, P.; Schettini, M. F.; Fortier, S.; Kaupp, M.; Hayton, T. W. *Angew. Chem., Int. Ed.* **2013**, *52*, 3259−3263.
(87) See for example: Vícha, J.; Straka, M.; Munzarová, M. L.; Marek, R. *J. Chem. Theory Comput.* **2014**, *10*, 1489−1499 and references therein.
(88) Autschbach, J. *J. Chem. Phys.* **2008**, *128*, 164112.
(89) Autschbach, J.; Zheng, S. *Magn. Reson. Chem.* **2008**, *46*, S45−S55.
(90) Bagno, A.; Saielli, G. *Theor. Chem. Acc.* **2007**, *117*, 603−619.

DOI: 10.1021/acs.inorgchem.5b00627
Inorg. Chem. 2015, 54, 5855−5863